


Effect of Pregnancy on Unbound Raltegravir Concentrations in the ANRS 160 RalFe Trial

Yi Zheng,^{a,b}  Déborah Hirt,^{a,b,c} Sandrine Delmas,^d Gabrielle Lui,^{a,b} Sihem Benaboud,^{a,b} Jerome Lechedanec,^d Jean-Marc Tréluyer,^{a,b,e} Camille Chenevier-Gobeaux,^f Elisa Arezes,^d Ambre Gelley,^g Imane Amri,^g Saïk Urien,^{b,e,h} Naïm Bouazza,^{b,e,h} Frantz Foissac,^{b,e,h} Josiane Warszawski,^{c,d} Jade Ghosn,^{i,j} for the ANRS 160 RalFe Study Group

^aService de Pharmacologie Clinique, AP-HP, Hôpital Cochin, Paris, France

^bEA7323, Université de Paris, Paris, France

^cInserm 1018 CESP, Hôpital Bicêtre, Le Kremlin-Bicêtre, France

^dService d'Epidémiologie et Santé Publique, AP-HP, Hôpital Bicêtre, Le Kremlin-Bicêtre, France

^eUnité de Recherche Clinique Paris Descartes Necker Cochin, AP-HP, Paris, France

^fService de Diagnostic Biologique Automatisé, AP-HP, Hôpital Cochin, Paris, France

^gANRS, France Recherche Nord&Sud Sida-hiv Hépatites, Paris, France

^hCIC-1419 Inserm, Cochin-Necker, Paris, France

ⁱService des Maladies Infectieuses et Tropicales, AP-HP, Hôpitaux Universitaires Paris Nord Val de Seine, site Bichat-Claude Bernard, Paris, France

^jINSERM UMR 1137 IAME, Université Paris Diderot, Faculté de Médecine site Bichat, Paris, France

ABSTRACT A population pharmacokinetic model was developed to explore the pharmacokinetics modification of unbound raltegravir during pregnancy. The RalFe ANRS160 study was a nonrandomized, open-label, multicenter trial enrolling HIV-infected pregnant women receiving a combined antiretroviral regimen containing 400 mg raltegravir twice daily. Biological samples were collected during the third trimester of pregnancy (between 30 and 37 weeks of gestational age) and at postpartum (4 to 6 weeks after delivery). A population pharmacokinetic model was developed with Monolix software. A total of 360 plasma samples were collected from 43 women during pregnancy and postpartum. The unbound raltegravir was described by a one-compartment model with a transit compartment with first-order absorption, evolving to bound raltegravir (by a linear binding to albumin) or metabolism to RAL-glucuronide or to a first-order elimination, with a circadian rhythm. During pregnancy, the absorption was decreased and delayed and the raltegravir elimination clearance and glucuronidation increased by 37%. Median total and unbound area under the curve from 0 to 12 h significantly decreased by 36% and 27% during pregnancy. Median total trough concentration (C_{trough}) decreased significantly in the evening (28%); however, the median total C_{trough} in the morning, unbound C_{trough} in the morning, and unbound C_{trough} in the evening showed a nonsignificant decrease of 16%, 1%, and 15%, respectively, during pregnancy compared to the postpartum period. This is the first study reporting the pharmacokinetics of unbound raltegravir during pregnancy. As unbound C_{trough} did not significantly decrease during the third trimester, the pregnancy effect on raltegravir unbound concentrations was not considered clinically relevant. (This study has been registered at ClinicalTrials.gov under identifier NCT02099474.)

KEYWORDS raltegravir, population pharmacokinetics, pregnant women, unbound concentrations, HIV

Mother-to-child transmission (MTCT) contributes to 9% of new HIV infections (1). Zero new HIV infections in infants by 2020 is one of the three new global health aims on HIV endorsed by the World Health Assembly in 2016 (1). To achieve this goal,

Citation Zheng Y, Hirt D, Delmas S, Lui G, Benaboud S, Lechedanec J, Tréluyer J-M, Chenevier-Gobeaux C, Arezes E, Gelley A, Amri I, Urien S, Bouazza N, Foissac F, Warszawski J, Ghosn J, for the ANRS 160 RalFe Study Group. 2020. Effect of pregnancy on unbound raltegravir concentrations in the ANRS 160 RalFe trial. *Antimicrob Agents Chemother* 64:e00759-20. <https://doi.org/10.1128/AAC.00759-20>.

Copyright © 2020 American Society for Microbiology. All Rights Reserved.

Address correspondence to Déborah Hirt, deborah.hirt@aphp.fr.

Received 26 April 2020

Returned for modification 12 June 2020

Accepted 6 July 2020

Accepted manuscript posted online 13 July 2020

Published 21 September 2020

access to combined antiretroviral therapy (cART) is key, being highly effective for the prevention of mother-to-child transmission (PMTCT) of HIV (2–5). One of the most important goals of cART is to decrease the level of plasma viral load, which is directly proportional to the risk of vertical transmission and to maternal morbidity and mortality (6, 7). With cART, the rate of MTCT falls from 15 to 40% to less than 2% (6, 8, 9).

Raltegravir (RAL) is the first HIV-1 integrase strand transfer inhibitor (INSTI), approved by the FDA in 2007. RAL monotherapy yields a drop in viral load ranging from -1.7 to $-2.2 \log_{10}$ copies/ml within 2 weeks compared to $-0.2 \log_{10}$ copies/ml in the placebo group (10, 11). Markowitz and colleagues also showed that plasma viral load decreased much more quickly with fewer adverse events in patients treated with a RAL-based cART compared to those treated with an efavirenz-based cART (12). Thus, RAL seems an appealing antiretroviral candidate for women living with HIV and presenting late during pregnancy, as it is paramount to decrease their plasma viral load as quickly as possible in such a setting.

Raltegravir is a P-glycoprotein (P-gp) substrate; it is primarily metabolized by the UGT1A1 isoenzyme to raltegravir-glucuronide metabolite. Physiological changes during pregnancy, especially during the third trimester of pregnancy (T3), are known to affect significantly the pharmacokinetics of drugs via absorption, distribution, metabolism, and excretion (delayed gastric emptying, increased gastric pH, increased intravascular and extravascular water content, increase enzyme activity, increased renal blood flow, etc.) (13–15). These changes could lead to a decrease in drug concentrations, lowering its effect. For these reasons, it is important to understand the change of RAL pharmacokinetics in pregnant women during T3.

Until now, scant RAL pharmacokinetics data from pregnant women were available. A phase 4 trial (PANNA study) reported a mean decrease of 29% of RAL area under the concentration-time curve from 0 to 12 h (AUC_{0-12}) in 17 HIV-infected pregnant women monitored during pregnancy and postpartum (16). However, this decrease was not consistent for all pregnant women, as 35% of them had a higher AUC_{0-12} during T3 (16). Another RAL pharmacokinetics study (IMPAACT 1026s) reported, in 38 women, an approximately 50% decrease in AUC_{0-12} during pregnancy (17). Moreover, a wide variability of RAL exposure was reported during T3 in previous studies (16, 17). Blonk et al. have reported a geometric mean AUC of 5,000 ng·h/ml with 95% confidence interval between 3,560 and 7,010 ng·h/ml for the women during the third trimester in the PANNA study. In the IMPAACT 1026s study, Watts et al. have shown an AUC ranging from 1,400–3,560 ng·h/ml for women during the third trimester. RAL has a large food effect; thus, the concomitant food intake could contribute to the differences observed between these 2 studies. In the PANNA study, RAL intake was done after a standard breakfast (650 kcal; 30 g fat), whereas in the IMPAACT study, women were required to fast for 2 h before and 2 h after the observed raltegravir dose. Based on total concentrations, both studies concluded that RAL dosage does not need to be modified during pregnancy. Of note, in both studies, concomitant medications that could modify RAL exposure were used for several patients, such as ritonavir-boosted atazanavir (4 patients in the PANNA study and 2 patients in the IMPAACT 1026s study). In addition, no data on proton pump inhibitor use were available in either study. Furthermore, genetic polymorphism of UGT1A1 (18) and P-glycoprotein (P-gp) (19–21) impacts the pharmacokinetics of RAL, and this was not taken into account in those clinical studies (16, 17).

For pregnant women, scarce data are available for pharmacokinetics of unbound RAL, which is considered the active fraction of RAL. RAL highly binds to human serum albumin (HSA) (83%) (22, 41). Thus, the decrease in plasma protein concentration reported during pregnancy could lead to an increase in the unbound fraction of RAL (24, 25).

The aim of this study was to assess the pharmacokinetics of unbound, total, and glucuronide RAL in pregnant women and to evaluate the influence of pregnancy and genetics on its pharmacokinetics.

TABLE 1 Participants' characteristics^f

| Parameter | Value |
|--|---|
| Median age at delivery (range) | 33 yr (23–45) |
| Nationality (<i>n</i> ^a) | |
| Sub-Saharan Africa | 72% (31) |
| France | 16% (7) |
| Haiti-Portugal-Switzerland | 12% (5) |
| Tobacco consumer (<i>n</i>) | 12% (5) |
| Alcohol consumer (<i>n</i>) | 0% (0) |
| Drug consumer (<i>n</i>) | 0% (0) |
| Start of raltegravir | |
| At the moment of conception (<i>n</i>) | 44% (18) |
| If not, the median GA (range) at start RAL | 20 (2–34) wk |
| Concomitant ARVs (<i>n</i>) | |
| NRTI | 7% (3) 3TC 10% (4) 3TC+ABC 49% (20) TDF+FTC |
| NRTI + PI | 2% (1) 3TC + DRV/r 12% (5) TDF+FTC+DRV/r |
| NNRTI | 2% (1) ETV |
| NNRTI + PI | 2% (1) ETV+ DRV/r |
| NRTI + NNRTI | 2% (1) TDF+NVP |
| PI | 12% (5) DRV/r |
| Inclusion at T3 (day 0) (<i>n</i> = 43) | |
| Gestation age, wk, median (range) | 33 (30–37) |
| Weight, kg, median (IQR) | 78.5 (69–86) |
| HIV RNA > 20 copies/ml ^b | 15% (6) |
| If HIV RNA > 20 copies/ml, median viral load (IQR) | 52 (40–90) copies/ml |
| CD4 count, cells/μl, median (IQR) | 539 (347–682) |
| Delivery (<i>n</i> = 43) | |
| Gestation age, wk, median (IQR) | 39 (39–40) |
| Cesarean delivery | 37% (16) |
| HIV RNA > 20 copies/ml at delivery ^c | 12% (5) |
| If HIV RNA > 20 copies/ml at delivery, median viral load (IQR) | 42 (40–68) copies/ml |
| CD4 count, cells/μl, median (IQR) ^d | 599 (459–789) |
| Postpartum (<i>n</i> = 39) | |
| Time after delivery, weeks, median (IQR) | 5 (4–5) |
| Weight, kg, median (IQR) | 70 (62–80) |
| HIV RNA > 20 copies/ml | 18% (7) |
| If HIV RNA > 20 copies/ml, median viral load (IQR) | 58 (40–2,230) copies/ml |
| CD4 count, cells/μl, median (IQR) | 609 (439–746) |
| Pregnancy outcomes (<i>n</i> = 41) | |
| Moderate premature ^e | 5% (2) |
| Birth weight, g, median (IQR) | 3,210 (2,840–3,450) |
| Infant HIV DNA and/or RNA PCR test negative | 100% (41) |

^a*n*, number of patients.^bData available for 37 patients.^cData available for 42 patients.^dData available for 39 patients.^eGestation ages between 32 to 36 weeks.^fAbbreviations: nucleoside analog reverse transcriptase inhibitor (NRTI), protease inhibitor (PI), nonnucleoside reverse transcriptase inhibitor (NNRTI), lamivudine (3TC), abacavir (ABC), tenofovir (TDF), emtricitabine (FTC), ritonavir boosted darunavir (DRV/r), etravirine (ETV), nevirapine (NEV), interquartile range (IQR).

RESULTS

Population characteristics. Forty-three pregnant women were included. For two women, the genotyping result of UGT1A1 was not available. Median (range) age was 33 (23 to 45) years, and the median (range) body weight was 78.5 (69 to 86) kg. More demographic characteristics are summarized in Table 1. The 43 women had blood

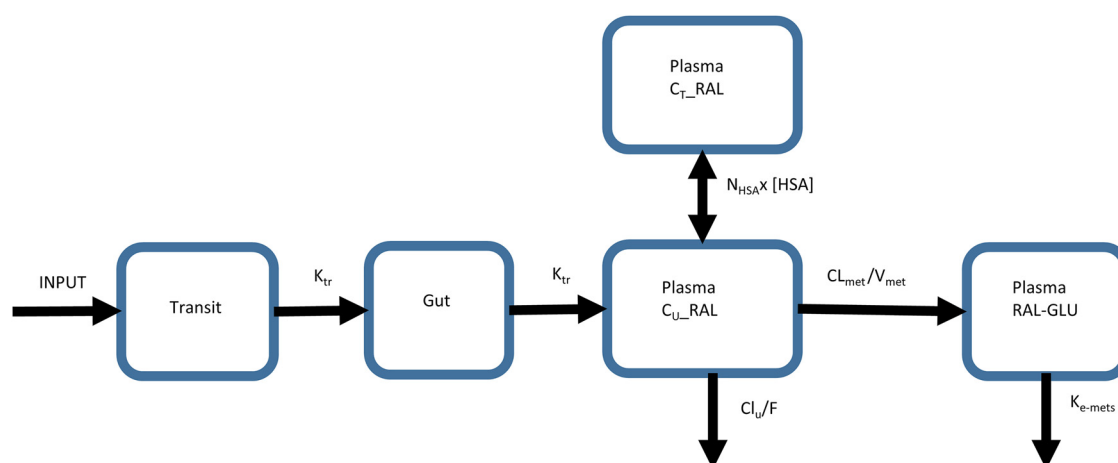


FIG 1 Population pharmacokinetic model of unbound, total, and glucuronide RAL concentrations. In this model, C_U -RAL, C_T -RAL, and C_{RAL-G} represent the unbound, total, and glucuronide-RAL concentration in plasma. The parameters estimated were the transit/absorption constant rate (K_{tr}), apparent elimination clearance of unbound RAL (CL_U/F), apparent volume of distribution of unbound RAL (V_U/F), transfer from unbound RAL to RAL-GLU (CL_{met}/V_{met}), elimination rate constant of RAL-GLU (K_{e-met}), N_{HSA} , number of drug binding sites in each molecule of HAS ($C_{BOUND} = N_{HSA} \cdot C_U \cdot [HSA]$), and the number of RAL binding sites in HSA. $[HSA]$ is the concentration of HSA in plasma.

sampling during T3, and 39 of them had blood sampling during the postpartum period. A total of 360 plasma samples were collected, allowing for quantification of 360 total RAL, 360 RAL-glucuronide (RAL-GLU), and 354 unbound RAL. Due to insufficient volume, six plasma samples could be used to determine the concentrations of total RAL and RAL-GLU but not unbound RAL. All concentrations were collected at steady state. Only one unbound, one total, and one glucuronide concentration were below the lower limit of quantification (LLOQ), so they were set to half the LLOQ.

The genotyping result of P-gp was available for 39 women. The percentages of wild-type homozygotes, heterozygotes, and mutant homozygotes of P-gp were 74.35% ($n = 29$), 17.95% ($n = 7$), and 7.69% ($n = 3$), respectively. For UGT1A1, 41 results were available: 24.39% of women ($n = 10$) were wild type with (TA)6/(TA)6, 2.44% of women ($n = 1$) with (TA)5/(TA)6, 2.44% of women ($n = 1$) with (TA)5/(TA)7, 39.02% of women ($n = 16$) with (TA)6/(TA)7, 2.44% of women ($n = 1$) with (TA)6/(TA)8, 26.83% of women ($n = 11$) with (TA)7/(TA)7, and 2.44% of women ($n = 1$) with (TA)7/(TA)9.

Population pharmacokinetic modeling. A one-compartment model, with first-order absorption and elimination, best described the mother's unbound RAL concentrations. A transit compartment was added to mimic the delayed arrival of the drug in plasma. Finally, K_a and the transit time constant (K_{tr}) were confounded to a unique absorption parameter ($K_a = K_{tr}$). As RAL was mostly bound to HSA, the total RAL concentrations (C_T) were related to the unbound RAL concentrations (C_U) according to a nonspecific (linear) binding to HSA, i.e., $C_T = C_U \cdot (1 + N_{HSA} \cdot [HSA])$. A nonlinear binding was also tested but did not improve the model. An additional compartment was added to describe the RAL-GLU formation from RAL.

The final combined pharmacokinetic model for unbound RAL, total RAL, and RAL-GLU is graphically represented in Fig. 1. The pharmacokinetic parameters estimated were the transit/absorption rate constant (K_{tr}), apparent elimination clearance of unbound RAL (CL_U/F), apparent volume of distribution of unbound RAL (V_U/F), transfer from unbound RAL to RAL-GLU (CL_{met}/V_{met}), elimination constant rate of RAL-GLU (k_{e-mets}), and the number of RAL binding sites in HSA (N_{HSA}). A cosine function was used to represent the circadian rhythm of RAL elimination, as already proposed for nevirapine (23). This function was added on both CL_U/F and CL_{met}/V_{met} , the amplitude of the cosine oscillation, AMP, was estimated, and the phase shift of the cosine function was fixed to midnight. To prevent negative values of clearances, the effect of the circadian

TABLE 2 Parameters estimated of the final unbound, total, and glucuronide-raltegravir population model in 43 women during the third trimester pregnancy and postpartum^a

| Parameter | Estimate | RSE% |
|---|----------|------|
| K_{TR} (h^{-1}) | 2.78 | 16 |
| CL_U/F (liters· h^{-1}) | 130 | 11 |
| V_U/F (liters) | 1710 | 16 |
| CL_{met}/V_{met} (h^{-1}) | 5.17 | 27 |
| K_{e-mets} (h^{-1}) | 2.45 | 25 |
| N_{HSA} | 0.102 | 6 |
| β^{preg} on K | 0.225 | 6 |
| β^{preg} on CL_U/F and CL_{met}/V_{met} | 1.37 | 3 |
| β^{Amp} on CL_U/F and CL_{met}/V_{met} | 0.212 | 4 |
| $Corr_V_U/F_CL_U/F$ | 0.877 | 5 |
| $\omega_{K_{TR}}$ | 0.887 | 12 |
| $\omega_{CL_U/F}$ | 0.631 | 12 |
| $\omega_{V_U/F}$ | 0.973 | 12 |
| $\omega_{CL_{met}/V_{met}}$ | 0.447 | 15 |
| RPE-unbound | 0.63 | 4 |
| RPE-total | 0.648 | 5 |
| RPE-metabolite | 0.628 | 5 |

^aRSE%, relative standard error, derived from the covariance matrix; K_{TR} , transition rate/absorption rate; CL_U , clearance of unbound fraction of RAL; V_U , central volumes of distribution of unbound fraction of RAL; CL_{met} , clearance of RAL metabolized into RAL-glucuronide; V_{met} , volume of distribution of RAL-glucuronide; K_{e-mets} , elimination rate of RAL-glucuronide; N_{HSA} , number of drug binding sites in each molecule of human serum albumin ($C_{BOUND} = N_{HSA} \cdot C_U \cdot HSA$); $\beta^{K/preg}$, the effect of pregnancy on absorption rate of unbound fraction of RAL; β^{preg} on CL_U/F and CL_{met}/V_{met} , the effect of pregnancy on clearance of unbound fraction of RAL and on RAL glucuronidation; β^{Amp} on CL_U/F and CL_{met}/V_{met} , the amplitude of the cosine oscillation on clearance of unbound fraction of RAL and on RAL glucuronidation (the phase shift of the cosine function was fixed to 00:00); ω , between-subject variability; RPE, residual proportional error; F, bioavailability. The pregnant effect on the K_{TR} , CL_U/F , and CL_{met}/V_{met} and circadian rhythm effect on CL_U/F and CL_{met}/V_{met} were obtained using the following equations: $K_{TR} = 2.78 \times (0.225)^{PREG}$, $\frac{CL_U}{F} = 130 \times (1.37)^{PREG} \times e^{0.212 \times \frac{2\pi}{24} \times t_{mi}}$, $\frac{CL_{met}}{V_{met}} = 5.17 \times (1.37)^{PREG} \times e^{0.212 \times \frac{2\pi}{24} \times t_{mi}}$, where PREG = 1 if samples were collected during pregnancy and 0 if otherwise.

rhythm was modeled as exponential and could be interpreted approximately as a relative change.

Models with separate additive errors, proportional errors, or mixed errors were tested, and the most suitable models were proportional error models. The between-subject variability was estimated for K_{TR} , CL_U/F , V_U/F , and CL_{met}/V_{met} . The inclusion of the cosine function decreased the objective function value (OFV) by 195 U, and then the addition of the pregnant effect on the K_{TR} led to a decrease of 99 U in the objective function value and 17% in the K_{TR} intersubject variability. In pregnant women, K_{TR} was multiplied by 0.225 (95% inhibitory concentration [IC_{95}], 0.198 to 0.256). The inclusion of pregnancy effect on both CL_U/F and CL_{met}/V_{met} led to a decrease of 19 U in the objective function value (10 U for each inclusion) and 3% in both the CL_U/F intersubject variability and CL_{met}/V_{met} intersubject variability. In pregnant women, these clearances were multiplied by 1.37 (IC_{95} , 1.29 to 1.46). Both the allometric scaling and the effect of bodyweight on clearance and volume were tested, but the objective function value did not decrease significantly. After inclusion of these covariates, no other covariate had a significant effect on RAL pharmacokinetics. The final population pharmacokinetics parameters are summarized in Table 2, and the population pharmacokinetic curves for unbound, total, and glucuronide RAL are represented in Fig. 2. Pregnant women were found to have a K_{TR} of 77% lower, resulting in a delayed absorption of the drug. Pregnant women had a higher clearance (37%) than the nonpregnant women, resulting in a faster elimination (Fig. 2).

The visual predictive check showed that the 5th, 50th, and 95th percentiles of the observed data were well within the 90% confidence intervals of the 5th, 50th, and 95th percentiles of the simulated concentrations (Fig. 3).

Pharmacokinetic comparisons between pregnant and nonpregnant women.

The median (range) HSA plasma concentration was 33.2 g/liter (19.4 to 49.5 g/liter) during T3 and 41.2 g/liter (22.9 to 56.2 g/liter) during postpartum, representing a

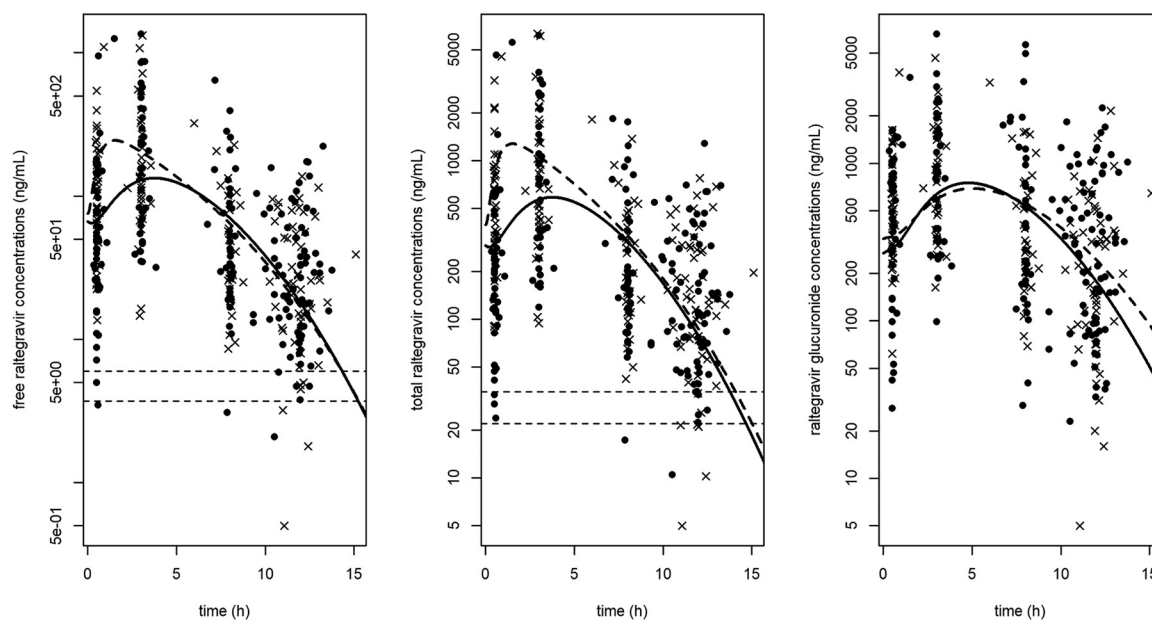


FIG 2 Observed raltegravir unbound concentration, total concentration and glucuronide concentration (from left to right) and population median predictions (dashed curve for the nonpregnant women and solid curve for the pregnant women) for each fraction obtained from the pharmacokinetic model proposed. The points and the full curve represent the concentration obtained during pregnancy, and the crosses and dashed curve represent the concentration obtained during postpartum. The horizontal lines correspond to 35 and 22 ng/ml for total raltegravir and 6 and 3.7 for unbound raltegravir.

median intraindividual decrease of 17% in the third trimester of pregnancy. The median unbound fraction (f_u) was 22.5% during T3 and 19.2% during postpartum, representing a median intraindividual increase of 3% during pregnancy. Areas under the curve, trough concentrations, and paired Wilcoxon tests are reported in Table 3. A median

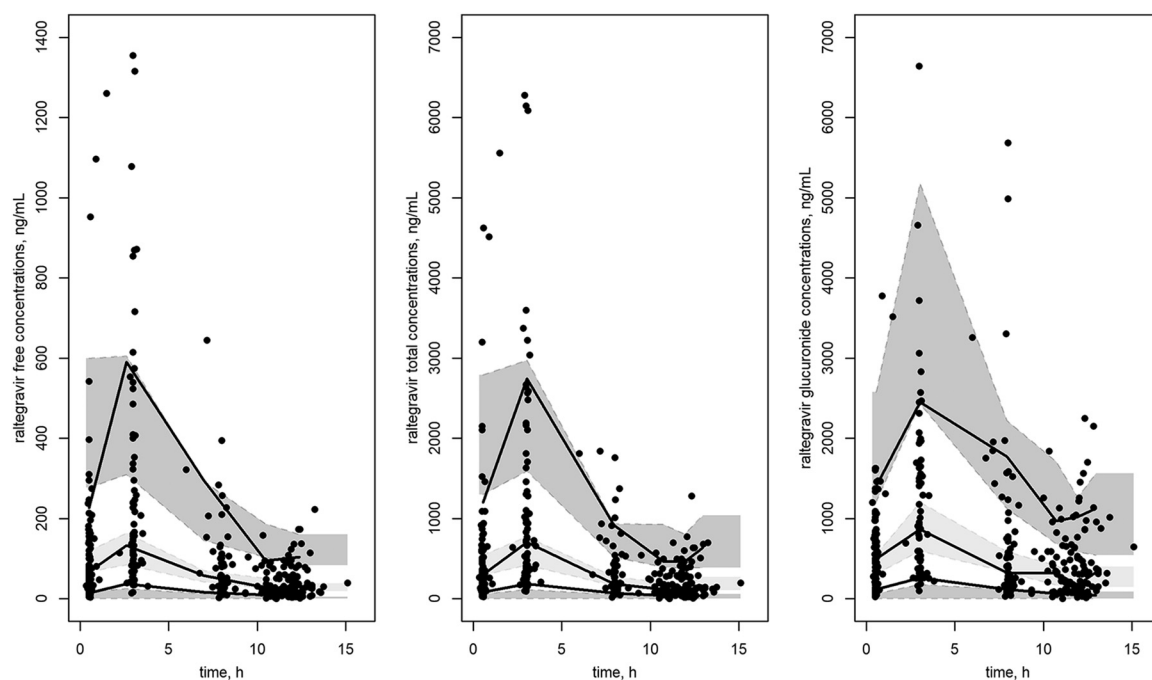


FIG 3 Visual predictive check (VPC) plots for evaluation of the pharmacokinetic model of raltegravir unbound fraction (left), total fraction (center), and glucuronide fraction (right). The lines show the 5th, 50th, and 95th percentiles of observed data. The areas represent the 90% confidence interval around the simulated percentiles. Blue-filled circles stand for observed concentrations of RAL for each fraction.

TABLE 3 Daily and nightly unbound, total, and glucuronide-raltegravir areas under the curve and trough concentrations for pregnant and postpartum women

| Parameter | Median (range) value for: | | |
|---|-------------------------------------|----------------------|-------------------------------|
| | 3rd trimester of pregnancy (N = 43) | Postpartum (N = 39) | Wilcoxon paired test (N = 39) |
| AUC _{8–20hr} C _{trough} evening | | | |
| Unbound AUC (ng·h/ml) | 853 (204–3,298) | 1,292 (273–4,174) | $P < 10^{-6}$ |
| Total AUC (ng·h/ml) | 3,921 (699–14,706) | 6,770 (1,506–21,859) | $P < 10^{-6}$ |
| Glucuronide AUC (ng·h/ml) | 5,175 (2,169–216,977) | 3,938 (1,073–15,362) | $P < 10^{-3}$ |
| Unbound C _{trough} (ng/ml) | 14 (1–86) | 13 (1–77) | $P = 0.12$ |
| Total C _{trough} (ng/ml) | 57 (3–277) | 69 (5–248) | $P < 10^{-5}$ |
| Glucuronide C _{trough} (ng/ml) | 149 (10–898) | 102 (11–385) | $P < 10^{-5}$ |
| AUC _{20–8hr} C _{trough} morning | | | |
| Unbound AUC (ng·h/ml) | 1,212 (278–4,263) | 1,725 (379–5,617) | $P < 10^{-6}$ |
| Total AUC (ng·h/ml) | 5,359 (956–18,614) | 9,209 (2,095–29,414) | $P < 10^{-6}$ |
| Glucuronide AUC (ng·h/ml) | 5,254 (281–24,669) | 4,122 (1,595–16,228) | $P = 0.33$ |
| Unbound C _{trough} (ng/ml) | 56 (8–176) | 65 (12–219) | $P = 0.26$ |
| Total C _{trough} (ng/ml) | 253 (37–605) | 321 (63–931) | $P = 0.84$ |
| Glucuronide C _{trough} (ng/ml) | 269 (38–880) | 207 (55–795) | $P < 10^{-4}$ |

intraindividual decrease of 36% for total AUC_{0–12} and 27% for unbound AUC_{0–12} was observed in pregnant women compared to nonpregnant women. Unbound and total AUC_{0–12} were significantly lower in pregnant women than in nonpregnant women during the day and during the night ($P < 10^{-6}$). For the concentration at 12 h (C₁₂), median intraindividual total RAL decreased in pregnant compared to nonpregnant women (16% in the morning and 28% in the evening); thus, the decrease was not significant in the morning but it was in the evening. The decrease in unbound C₁₂ was less pronounced (1% decrease in the morning and 15% in the evening) and was not significantly different between the 3rd trimester of pregnancy and postpartum, in the morning, or in the evening. A self-administered questionnaire was given to the mothers, and no suboptimal adherence was reported.

As shown in Fig. 2, for total trough RAL, seven samples from nonpregnant and nine from pregnant women (among 354) were below 35 ng/ml; for unbound trough RAL, six samples from nonpregnant and eight from pregnant women were below 6 ng/ml. Using the target of 22 ng/ml for total raltegravir, two samples from pregnant and five samples for nonpregnant women were below this value, and three samples from pregnant and three samples from nonpregnant women were below 3.7 ng/ml for the free fractions.

Clinical outcomes. Plasma HIV-RNA was below 20 copies/ml in 88% of participant women at delivery. HIV-RNA was above LLOQ in six women at delivery, with a median of 42 copies/ml, and amplification failed. All 41 infants tested negative for HIV at month 6. Eight adverse events were reported in seven women, but none was considered to be related to the use of RAL. The accountability for RAL was ruled out either because it was introduced after the 1st trimester of pregnancy or because the adverse event was clearly related to another identified etiology. The only grade 3 event was pregnancy cholestasis. Congenital abnormalities were reported for four infants (hexadactyly, agenesis of right kidney and duplicated vagina, hypoplasia of left thumb, and duplicated digestive tract in iliac fossa), and five infants (12%) were hospitalized for six adverse events. However, these birth defects were not considered related to the use of RAL. Thus, RAL (400 mg twice a day) was considered well tolerated by pregnant women in this study.

DISCUSSION

This is the first population pharmacokinetic model describing unbound, total, and glucuronide RAL concentrations in pregnant women. This population approach is particularly useful in pregnant women, for whom it is difficult to collect many samples for a sufficiently large sample of women to correctly describe the high variability of this drug.

To date, only limited RAL pharmacokinetics data are available for pregnant women. In our study, during T3, mean total C_{trough} in the evening and daily AUC_{0-12} were 57 ng/ml and 3,921 ng·h/ml, corresponding to a decrease of 28 and 36%, respectively, compared to the postpartum period. This is in keeping with previous studies. In the PANNA study, the median C_{trough} and AUC_{0-12} were 77 ng/ml and 5,000 ng·h/ml during T3, with a mean decrease of 36% and 29% compared to postpartum (16). In the IMPAACT 1026s study, during T3, the median C_{trough} and AUC_{0-12} were 64 ng/ml and 5,400 ng·h/ml, with a mean decrease of 20% and 53% compared to postpartum levels (17).

RAL is 83% plasma protein bound, mostly to the HSA (23). As HSA is known to decrease during pregnancy (26), f_u of RAL is expected to increase. Furthermore, unbound antiretrovirals are considered the active form, which could cross physiological/anatomical barriers (23, 27). Thus, unbound RAL should be analyzed for pregnant women; however, all previous studies focused only on the pharmacokinetics of total RAL, which may be less informative.

In the ANRS 160 RalFe trial, the median percentage of f_u was 22.5% during T3 and 19.2% during postpartum. This finding was not different from those of previous results (26.2% in healthy volunteers and 23.8% in HIV-infected patients) (23). The decrease in unbound RAL exposure during pregnancy is less pronounced than the decrease in total exposure; a mean decrease of 36% for total AUC_{0-12} and 27% for unbound AUC_{0-12} was observed in pregnant women compared to nonpregnant women. Median total C_{trough} decreased significantly in the evening (28%); however, median total C_{trough} in the morning, unbound C_{trough} in the morning, and unbound C_{trough} in the evening showed a nonsignificant decrease of 16%, 1%, and 15%, respectively, during pregnancy compared to the postpartum period. Thus, the dosage should not be modified during pregnancy.

In our study, pregnant women were found to have a lower absorption/transit constant rate (K_{TR} was 77% lower), corresponding to a lower C_{max} and a delayed absorption. While a decrease in C_{max} has also been reported in previous studies (16, 17), the delayed absorption was not observed in these studies. However, Watts et al. also observed an absorption lag time in about a third of pregnant women (17), which was in keeping with the results presented here. Furthermore, as a substrate of P-gp, the absorption of RAL might be reduced by increased expression of intestinal P-gp during pregnancy (21, 28, 29). Pregnancy-associated delayed gastric emptying and reduced small intestine motility could enhance this decrease of RAL absorption (15, 30). Nausea and vomiting could also lead to a reduced absorption of RAL (15).

Pregnant women were found to have a 37% increase in both CL_{U}/F and $CL_{\text{met}}/V_{\text{met}}$, reflecting increased RAL glucuronidation, increased elimination of the unbound RAL, and/or decreased bioavailability. Indeed, RAL was shown to be primarily metabolized by the UGT1A1 isoenzyme (31). In previous studies, UGT1A1 activity was found to be increased during pregnancy due to increased cortisol and progesterone levels (32, 33). Moreover, RAL is 9% eliminated unchanged in urine, and the glomerular filtration rate is known to be increased during pregnancy. Finally, RAL is the substrate of P-gp, which is more expressed during pregnancy and could result in an increased efflux of RAL (decreasing bioavailability) (28).

Several limitations can be cited. Pregnancy could only be added as a dichotomous variable, as pregnant women were only seen at the third trimester of pregnancy (between 30 and 37 weeks of gestational age), and the effect of pregnancy on absorption could have been estimated more accurately, avoiding the gap of sample collection between 0.5 h and 3 h. A PFIM optimization based on a published model for total RAL was performed before the study to choose the sampling time (predose and 0.5, 3, 8, and 12 h after administration). However, we built a more complex model with additional points in the elimination phase that may have improved our model and the determination of other clearance covariates.

In conclusion, this is the first population pharmacokinetic model describing unbound, total, and glucuronide RAL concentrations in pregnant women. During T3,

median total C_{trough} and AUC_{0-12} decreased by 28% and 36% compared to levels during the postpartum period. Pregnant women were found to have a delayed and lower absorption of the drug and a 37% higher elimination than the nonpregnant women. Unbound C_{trough} values were not significantly different in women during their pregnancy and their postpartum period. However, concentrations in pregnant women did not fall below the target for effectiveness more often than that in nonpregnant women. As the unbound RAL concentrations were not found to be significantly impacted in pregnancy, these data further support the prior conclusions of PANNA and IMPAACT P1026s studies on total RAL exposure that no adjustment of the RAL dose for pregnant women is warranted.

MATERIALS AND METHODS

Patients. The RalFe ANRS 160 study (ClinicalTrials registration no. NCT02099474) was an open-label, multicenter, phase II, nonrandomized trial. All HIV-1-infected pregnant women included in this study were more than 18 years old and between 30 and 37 weeks of gestational age. The French Ethics Committee and the relevant authority approved this study, and a signed informed consent was obtained for all participating pregnant women.

Treatments. To be eligible, pregnant women enrolled had to be on a stable cART for at least 15 days before inclusion, containing RAL at the standard dosage (400 mg twice daily) by oral administration. Participating women could not receive atazanavir, fosamprenavir, efavirenz, rifampicin, phenobarbital, phenytoin, gastrointestinal topicals, antacids, adsorbents, or proton pump inhibitors, all of which have been shown to interact with RAL, as mentioned in the product information (34). RAL was given under supervision the days of the PK study; it was taken in the morning with a standard breakfast.

Sample collection. Five blood samples were collected at 0 (predose), 0.5 (H0.5), 3 (H3), 8 (H8), and 12 (H12) h after drug intake during T3 (between 30 and 37 weeks of gestational age) and in the postpartum period (between 4 and 6 weeks after delivery). All blood samples were collected into 5-ml EDTA vacutainer tubes. All blood samples were centrifuged at 4,000 rpm during 5 min at 4°C, within 8 h after sampling, and then plasma was stored at -80°C until analysis. An aliquot of blood sample for each woman was directly stored at -80°C for the extraction of DNAs and genotyping analysis. Plasma samples were used to determine RAL unbound, total, and glucuronide concentrations. HSA, alanine aminotransferase (ALAT), aspartate aminotransferase (ASAT), creatinine (CREA), and bilirubin (BILI) were measured during T3 and postpartum.

Analytical methods. RAL unbound, total, and glucuronide concentrations were measured in the clinical pharmacology department of Cochin Hospital (Paris, France). A liquid chromatography-tandem mass spectrometry (LC-MS/MS) method was used to determine the total and glucuronide RAL concentration, ranging from 10 (LLOQ) to 4,000 ng/ml for both (35). The unbound concentration of RAL was obtained by an ultrafiltration method using Centrifree ultrafiltration devices (molecular weight cutoff, 30 kDa) (Merck Millipore, Ireland) and then measured using a validated LC-MS/MS method with a calibration curve between 1 and 400 ng/ml for unbound raltegravir. The method was validated according to Food and Drug Administration (FDA) guidelines with the intra- and interday accuracy and precision inferior to 12% (36). The nonspecific binding effect was inferior to 6%, which could be considered negligible.

Genotyping. DNAs were extracted from total blood using a Qiagen Midi kit (France, Courtaboeuf) by following the manufacturer's instructions. Quality control and quantity were assessed with a NanoDrop (ThermoFisher).

The rs1045642 polymorphism in P-gp has been genotyped using the TaqMan predesigned kit (Life Technologies, Courtaboeuf) by following the manufacturer's instructions on an Applied Biosystems QuantStudio 5 real-time PCR system.

The polymorphism of TA repetition in the TATA box of UGT1A1, denoted rs8175347, has been sequenced using, in the first PCR step, the following primers (18832463; Ehmer): forward, 5'-AACATTA ACTTGGTGTATCGATTGGT-3'; reverse, 5'-AGCAGGCCAGGACAAGT-3'. PCR amplicons were then purified and sequenced by Eurofins (France) using the cycle sequencing technology (dideoxy chain termination/cycle sequencing) on ABI 3730XL sequencing machines and BigDye3.1 chemistry.

Population pharmacokinetic model. The modeling of RAL unbound, total, and glucuronide concentrations was performed using the software MONOLIX, version 2018R1 (<http://lixoft.com>).

The RAL unbound concentration was the first focus for model development, and then the RAL total concentration was fitted. Different models were tested for the RAL unbound concentrations (with one or two compartments, first-order absorption with lag time or with transit compartments, and first-order elimination with or without a cosine function to represent circadian rhythm). The total RAL concentrations were linked to the unbound concentrations by relationships integrating the HSA concentrations. Alternative relationships were examined by linear and nonlinear protein binding regression, as previously described (37). Lastly, the RAL-GLU concentration was added by the addition of another compartment, linked to the unbound compartment by a first-order constant. The residual variabilities of the model for unbound, total, and metabolite RAL were evaluated by testing several error models (additive, proportional, or mixed error model). The interindividual variabilities (IIV) were assumed to be a log-normal distribution.

Covariates (COV) included age, body weight, ASAT, ALAT, CREA, BILI, and pregnancy, and two genetic polymorphism (UGT1A1*28 and rs1045642 in P-gp) were investigated for developing the model. These

covariates were evaluated via upward-backward model building, as previously described (38). A covariate would be selected if (i) its effect was physiologically plausible, (ii) it could reduce the log-likelihood value by 6.63 U (χ^2 with 1 degree of freedom; $P < 0.01$) minimum for nested models or reduce the Akaike information criterion (AIC) and Bayesian information criteria (BIC) for nonnested models, (iii) it could reduce the variability of the pharmacokinetic parameter assessed based on the associated IIV, and (iv) it could improve diagnostic graphics.

For the test of genetic polymorphism effect, women were first split into the following two categories: homozygote wild type versus mutation type. Three categories (homozygote wild type, homozygote mutation, and heterozygote) were also tested for the effect of P-gp. For UGT1A1, the homozygote wild type was (TA)₆/(TA)₆ with 6 repetition of TA in the TATA box of the two alleles in UGT1A1 gene. It could mutate to (TA)₅, (TA)₇, or (TA)₈ with 5, 7, or 8 repetition of TA in one allele (heterozygote) or both (homozygote mutation) in the UGT1A1 gene (39). For P-gp, the homozygote wild type was C/C SNP in exon 26 of P-gp. The mutation type included C/T SNP (heterozygote) or T/T SNP (homozygote mutation) in exon 26 of P-gp (19).

Model evaluation. The goodness of fit of each model was evaluated by visual inspection of the observed-predicted (population and individual) concentration scatterplots. Diagnostic graphics and other statistics were obtained using R software. From the final model, 500 simulations were performed to compute the visual predictive check (VPC).

Pharmacokinetic comparisons between women during pregnancy and postpartum. Areas under the curve from 0 to 12 h (AUC_{0-12}) and trough concentrations (C_{12}) for the unbound, total, and glucuronide RAL were derived from the final model for the morning and for the evening administration. Wilcoxon paired test was used to compare these parameters during and after pregnancy. RAL total (and unbound) trough concentrations were also compared to 35 ng/ml, the estimated tenth percentile in nonpregnant historical controls, as proposed in the IMPAACT study (corresponding to 6 ng/ml for free fraction), and the target value of 22 ng/ml for total raltegravir (corresponding to 3.7 ng/ml for free fraction), derived from therapeutic drug monitoring, using a value derived from the ROC of Rizk et al (40).

ACKNOWLEDGMENTS

This work was supported and funded by Agence National de Recherche sur le Sida et les Hépatites Virales (ANRS AO 2015), with a grant from MSD France.

The participants in the ANRS 160 RalFe Study Group included Equipe EPF: CESP INSERM U1018, Le Kremlin-Bicêtre, France (M. Agen, E. Arezes, S. Delmas, A. Garin, P. Huyn, J. Le Chenadec, J. Warszawski); Hôpital Civil Strasbourg (David Rey); U1136, Paris, France (Dominique Costagliola); CHU Tours, France (Francis Barin); APHP Hôpital Avicenne, Bobigny, France (Yazid Baazia, Wael Mansour, Iwaka Valentin); APHP Hôpital Jean Verdier, Bondy, France (Amélie Benbara*, Lionel Carbillon, Catherine Delannoy, Marie-Florence Dzukam, Vincent Jeantils*, Mufide Kahraman, Eric Lachassine*, Oscar Lezcano, Fatouma Mchangama, Youssouf Mohamed Kassim); APHP Hôpital Bécélère, Clamart, France (Ghislaine Bachelet, Yves Castanet, Véronique Chambrin*, Laure Clech*, Anne Gaël Cordier*, Sylvie Cosse, Benjamin Deviaris, Sophie Nedellec, Salima Oucherif, Isabelle Poirrier, Mariem Raho-Moussa); APHP Hôpital Beaujon, Clichy, France (Maïa Banige, Christine Bazin, Mariam Bensalah, Pierre-François Ceccaldi*, Agnès Villemant Uludag*); APHP Hôpital Louis Mourier, Colombes, France (Martine Bloch, Catherine Crenn-Hebert, Dominique Duro, Corinne Floch-Tudal*, Houria Ichou, Laurent Mandelbrot, Laurence Marty, Fabienne Mazy, Françoise Meier*, Emmanuel Mortier); Centre Hospitalier Sud Francilien, Corbeil Essonne, France (Zaitoun Abdallah Moussa, Nouara Agher, Martine Blanchard, Amélie Chabrol*, Pierre Chevojon, Alain Devidas, Anne-Claire Donnadiou*, Dominique Fernandez, Michèle Granier*, Sabah Kubab, Joelle Neizelien, Rose Nguyen, Claire Malbrunot); Centre Hospitalier Intercommunal, Créteil, France (Jérôme Barré, Valérie Garrait*, Diane Jourdan, Christiane Kommé, Patrick Ledudal, Lanto Ratsimbazafy*, Laurent Richier); APHP Hôpital de Bicêtre, Le Kremlin-Bicêtre, France (Claire Boithias, Katia Bourdic, Claire Colmant*, Corinne Fourcade*, Sylvie Fridmann, Cécile Goujard*, Ikram Jrad, Laure Jule, Delphine Peretti*); Centre Hospitalier Intercommunal, Montreuil, France (Valérie Chety, Fatma Hamila, Brigitte Heller-Roussin*, Christophe Poncelet*, Hana Talabani-Boizot, Cécile Winter*); APHP Hôpital Bichat, Paris, France (Lahcene Allal, Mélanie Bertine, Marylène Bodard, Agnès Bourgeois Moine*, Sandrine Chendjou, Florence Damond, Sylvie Lariven, Sylvie Le Gac, Sophie Matheron*, Fabienne Mazy, Sarah Peerbaccus, Bao Phung, Adriana Pinto, Mandovi Rajguru, Julia Zelig); APHP Hôpital Cochin-Port Royal, Paris, France (Touria Belkacem, Sihem Benaboud, Alexandra Compagnucci, Ghislaine Firtion, Déborah Hirt, Anne Krivine, Gabrielle Lui, Yi Zheng, Valérie Marcou, Emmanuelle Pannier*, Jean-Marc Treluyer);

APHP Hôpital Européen Georges Pompidou, Paris, France (Lio Collias, Marina Karmochkine*, Hélène Peré, Marie-Laure Lucas, Magalie Ptak, Christelle Ledoux); APHP Hôpital Hôtel-Dieu, Paris, France (Agnès Cros, Jade Ghosn*, Maria Blanca Hadacek, Christophe Kokougan, Aline Maignan, Audrey Merlet, Thu Huyen Nguyen, Hafeda Rostane, Alain Sobel, Jean Paul Viard); APHP Hôpital Lariboisière, Paris, France (Dominique Ayrat, Guylaine Castor-Alexandre, Nicole Ciraru-Vigneron*, Véronique Delcey, Audrey Depond, Myriam Diemer, Geneviève Mouchnino, Anne Coursol, Agathe Rami*, Pierre Sellier, Safia Souak); APHP Hôpital Necker, Paris, France (Véronique Avettand, Stéphane Blanche*, Caroline Charlier, Claudine Duvivier*, Pierre Frange, Nathalie Kerguen, Delphine Lemerrier, Marine Driessen*, Adeline Melard, Christine Pichon, Claire Rouzaud, Fatima Touam, Florence Veber); APHP Groupe Hospitalier Pitié Salpêtrière, Paris, France (Henri Agut, Manuela Bonmarchand, Patricia Bourse, Erika Bourzam, Fabienne Caby, Vincent Calvez, Aziza Chermak, Marc Dommergues*, Catherine Lupin, Isabelle Melonio, Audrey Merlet, Marco Millones, Luminata Schneider, Anne Simon*, Jennifer Sommer, Cathia Soulie, Roland Tubiana*, Christine Blanc); APHP Hôpital Saint-Louis, Paris, France (Marie-Laure Chaix, Constance Delaugerre, Nadia Mahjoub); APHP Hôpital Tenon, Paris, France (Bassel Bachour, Valérie Berrebi, François Hervé*, Catherine Lependeven, Lise Selleret*, Laurence Slama*, Pélagie Thibaut, Loraine Zarka); APHP Hôpital Trousseau, Paris, France (Eida Bui, Bruno Carbonne, Catherine Dollfus*, Philippe Faucher*, Yanne Michel, Kendra Saloum, Aurélie Schnurgier, Marie-Dominique Tabone, Geneviève Vaudre); APHP Hôpital Paul Brousse, Villejuif, France (Coralie Pallier, Muriel Mace, Lina Mouna); Centre Hospitalier Général, Saint-Denis, France (Sabrine Andris, Pascal Bolot*, Abdelghani Boussairi, Chantal Chaplain, Dieudonné Ekoukou, Nelly Ghibaud, Amel Mahdi*, Christelle Nourry, Isabelle Gros, Marie-Aude Khuong-Josses*). *, Principal investigator.

We have no conflicts of interest to declare.

REFERENCES

1. WHO. 2020. Global guidance on criteria and processes for validation: elimination of Mother-to-Child Transmission of HIV and Syphilis. World Health Organization, Geneva, Switzerland.
2. Cooper ER, Charurat M, Mofenson L, Hanson CI, Pitt J, Diaz C, Hayani K, Handelsman E, Smeriglio V, Hoff R, Blattner W, Group for the WITS. 2002. Combination antiretroviral strategies for the treatment of pregnant HIV-1-infected women and prevention of perinatal HIV-1 transmission. *J Acquir Immune Defic Syndr* 29:484. <https://doi.org/10.1097/00126334-200204150-00009>.
3. Townsend CL, Cortina-Borja M, Peckham CS, de Ruiter A, Lyall H, Tookey PA. 2008. Low rates of mother-to-child transmission of HIV following effective pregnancy interventions in the United Kingdom and Ireland, 2000–2006. *AIDS* 22:973–981. <https://doi.org/10.1097/QAD.0b013e3282f9b67a>.
4. Fowler MG, Qin M, Fiscus SA, Currier JS, Flynn PM, Chipato T, McIntyre J, Gnanashanmugam D, Siberry GK, Coletti AS, Taha TE, Klingman KL, Martinson FE, Owor M, Violar A, Moodley D, Theron GB, Bhosale R, Bobat R, Chi BH, Strehlau R, May P, Loftis AJ, Browning R, Fenton T, Purdue L, Basar M, Shapiro DE, Mofenson LM. 2016. Benefits and risks of antiretroviral therapy for perinatal HIV prevention. *N Engl J Med* 375:1726–1737. <https://doi.org/10.1056/NEJMoa1511691>.
5. Dabis F, Msellati P, Meda N, Welffens-Ekra C, You B, Manigart O, Leroy V, Simonon A, Cartoux M, Combe P, Ouangré A, Ramon R, Ky-Zerbo O, Montcho C, Salamon R, Rouzioux C, Van de Perre P, Mandelbrot L. 1999. 6-Month efficacy, tolerance, and acceptability of a short regimen of oral zidovudine to reduce vertical transmission of HIV in breastfed children in Côte d'Ivoire and Burkina Faso: a double-blind placebo-controlled multicentre trial. *Lancet* 353:786–792. [https://doi.org/10.1016/S0140-6736\(98\)11046-2](https://doi.org/10.1016/S0140-6736(98)11046-2).
6. Warszawski J, Tubiana R, Le Chenadec J, Blanche S, Teglas J-P, Dollfus C, Faye A, Burgard M, Rouzioux C, Mandelbrot L, ANRS French Perinatal Cohort. 2008. Mother-to-child HIV transmission despite antiretroviral therapy in the ANRS French Perinatal Cohort. *AIDS* 22:289–299. <https://doi.org/10.1097/QAD.0b013e3282f3d63c>.
7. Myer L, Essajee S, Broyles LN, Watts DH, Lesosky M, El-Sadr WM, Abrams EJ. 2017. Pregnant and breastfeeding women: a priority population for HIV viral load monitoring. *PLoS Med* 14:e1002375. <https://doi.org/10.1371/journal.pmed.1002375>.
8. Delicio AM, Lajos GJ, Amaral E, Lopes F, Cavichioli F, Miyoshi I, Milanez H. 2018. Adverse effects of antiretroviral therapy in pregnant women infected with HIV in Brazil from 2000 to 2015: a cohort study. *BMC Infect Dis* 18:485. <https://doi.org/10.1186/s12879-018-3397-x>.
9. Connor EM, Sperling RS, Gelber R, Kiselev P, Scott G, O'Sullivan MJ, VanDyke R, Bey M, Shearer W, Jacobson RL. 1994. Reduction of maternal-infant transmission of human immunodeficiency virus type 1 with zidovudine treatment. Pediatric AIDS Clinical Trials Group Protocol 076 Study Group. *N Engl J Med* 331:1173–1180. <https://doi.org/10.1056/NEJM199411033311801>.
10. Markowitz M, Morales-Ramirez JO, Nguyen B-Y, Kovacs CM, Steigbigel RT, Cooper DA, Liporace R, Schwartz R, Isaacs R, Gilde LR, Wenning L, Zhao J, Tepler H. 2006. Antiretroviral activity, pharmacokinetics, and tolerability of MK-0518, a novel inhibitor of HIV-1 integrase, dosed as monotherapy for 10 days in treatment-naïve HIV-1-infected individuals. *J Acquir Immune Defic Syndr* 43:509–515. <https://doi.org/10.1097/QAI.0b013e31802b4956>.
11. Grinsztejn B, Nguyen B-Y, Katlama C, Gatell JM, Lazzarin A, Vittecoq D, Gonzalez CJ, Chen J, Harvey CM, Isaacs RD. 2007. Safety and efficacy of the HIV-1 integrase inhibitor raltegravir (MK-0518) in treatment-experienced patients with multidrug-resistant virus: a phase II randomised controlled trial. *Lancet* 369:1261–1269. [https://doi.org/10.1016/S0140-6736\(07\)60597-2](https://doi.org/10.1016/S0140-6736(07)60597-2).
12. Markowitz M, Nguyen B-Y, Gotuzzo E, Mendo F, Ratanasuwana W, Kovacs C, Prada G, Morales-Ramirez JO, Crumpacker CS, Isaacs RD, Gilde LR, Wan H, Miller MD, Wenning LA, Tepler H, Protocol 004 Part II Study Team. 2007. Rapid and durable antiretroviral effect of the HIV-1 integrase inhibitor raltegravir as part of combination therapy in treatment-naïve patients with HIV-1 infection: results of a 48-week controlled study. *J Acquir Immune Defic Syndr* 46:125–133. <https://doi.org/10.1097/QAI.0b013e318157131c>.
13. Bailey H, Zash R, Rasi V, Thorne C. 2018. HIV treatment in pregnancy. *Lancet HIV* 5:e457–e467. [https://doi.org/10.1016/S2352-3018\(18\)30059-6](https://doi.org/10.1016/S2352-3018(18)30059-6).
14. Koren G, Pariente G. 2018. Pregnancy-associated changes in pharmacokinetics and their clinical implications. *Pharm Res* 35:61. <https://doi.org/10.1007/s11095-018-2352-2>.
15. Gilbert EM, Darin KM, Scarsi KK, McLaughlin MM. 2015. Antiretroviral

- pharmacokinetics in pregnant women. *Pharmacother J Hum Pharmacol Drug Ther* 35:838–855. <https://doi.org/10.1002/phar.1626>.
16. Blonk MI, Colbers APH, Hidalgo-Tenorio C, Kabeya K, Weizsäcker K, Haberl AE, Moltó J, Hawkins DA, van der Ende ME, Gengelmaier A, Taylor GP, Ivanovic J, Giaquinto C, Burger DM, van der Ven A, Nellen J, Lyons F, Lambert J, Wyen C, Faetkenheuer G, Rockstroh JK, Schwarze-Zander C, Sadiq ST, Gilleece Y, Wood C. 2015. Raltegravir in HIV-1-infected pregnant women: pharmacokinetics, safety, and efficacy. *Clin Infect Dis* 61:809–816. <https://doi.org/10.1093/cid/civ366>.
 17. Watts DH, Stek A, Best BM, Wang J, Capparelli EV, Cressey TR, Aweeka F, Lizak P, Kreitchmann R, Burchett SK, Shapiro DE, Hawkins E, Smith E, Mirochnick M, IMPAACT 1026s Study Team. 2014. Raltegravir pharmacokinetics during pregnancy. *J Acquir Immune Defic Syndr* 67:375–381. <https://doi.org/10.1097/QAI.0000000000000318>.
 18. Belkhir L, Seguin-Devaux C, Elens L, Pauly C, Gengler N, Schneider S, Ruelle J, Haufroid V, Vandercam B. 2018. Impact of UGT1A1 polymorphisms on raltegravir and its glucuronide plasma concentrations in a cohort of HIV-1 infected patients. *Sci Rep* 8:7359. <https://doi.org/10.1038/s41598-018-25803-z>.
 19. Hoffmeyer S, Burk O, von Richter O, Arnold HP, Brockmöller J, Johné A, Cascorbi I, Gerloff T, Roots I, Eichelbaum M, Brinkmann U. 2000. Functional polymorphisms of the human multidrug-resistance gene: multiple sequence variations and correlation of one allele with P-glycoprotein expression and activity in vivo. *Proc Natl Acad Sci U S A* 97:3473–3478. <https://doi.org/10.1073/pnas.050585397>.
 20. Hoque MT, Kis O, De Rosa MF, Bendayan R. 2015. Raltegravir permeability across blood-tissue barriers and the potential role of drug efflux transporters. *Antimicrob Agents Chemother* 59:2572–2582. <https://doi.org/10.1128/AAC.04594-14>.
 21. Minuesa G, Arimany-Nardi C, Erkizia I, Cedeño S, Moltó J, Clotet B, Pastor-Anglada M, Martínez-Picado J. 2016. Glycoprotein (ABC1) activity decreases raltegravir disposition in primary CD4+P-gp-high cells and correlates with HIV-1 viral load. *J Antimicrob Chemother* 71:2782–2792. <https://doi.org/10.1093/jac/dkw215>.
 22. Iwamoto M, Wenning LA, Petry AS, Laethem M, Smet MD, Kost JT, Merschman SA, Strohmaier KM, Ramael S, Lasseter KC, Stone JA, Gottesdiener KM, Wagner JA. 2008. Safety, tolerability, and pharmacokinetics of raltegravir after single and multiple doses in healthy subjects. *Clin Pharmacol Ther* 83:293–299. <https://doi.org/10.1038/sj.clpt.6100281>.
 23. Bienczak A, Cook A, Wiesner L, Mulenga V, Kityo C, Kekitiinwa A, Walker AS, Owen A, Gibb DM, Burger D, McIlleron H, Denti P. 2017. Effect of diurnal variation, CYP2B6 genotype and age on the pharmacokinetics of nevirapine in African children. *J Antimicrob Chemother* 72:190–199. <https://doi.org/10.1093/jac/dkw388>.
 24. Roustit M, Jlaiei M, Leclercq P, Stanke-Labesque F. 2008. Pharmacokinetics and therapeutic drug monitoring of antiretrovirals in pregnant women. *Br J Clin Pharmacol* 66:179–195. <https://doi.org/10.1111/j.1365-2125.2008.03220.x>.
 25. Metsu D, Toutain PL, Chatelut E, Delobel P, Gandia P. 2017. Antiretroviral unbound concentration during pregnancy: piece of interest in the puzzle? *J Antimicrob Chemother* 72:2407–2409. <https://doi.org/10.1093/jac/dkx176>.
 26. Abduljalil K, Furness P, Johnson TN, Rostami-Hodjegan A, Soltani H. 2012. Anatomical, physiological and metabolic changes with gestational age during normal pregnancy: a database for parameters required in physiologically based pharmacokinetic modelling. *Clin Pharmacokinet* 51:365–396. <https://doi.org/10.2165/11597440-000000000-00000>.
 27. Lê MP, Belarbi L, Chaix M-L, Dulioust E, Mahjoub N, Salmon D, Viard J-P, Duvivier C, Peytavin G, Launay O, Ghosn J. 2017. Penetration and antiviral efficacy of total and unbound maraviroc, raltegravir and rilpivirine in both female and male genital fluids from HIV-positive patients receiving regimens containing these antiretrovirals. *J Antimicrob Chemother* 72:3167–3171. <https://doi.org/10.1093/jac/dkx275>.
 28. Hashiguchi Y, Hamada A, Shinohara T, Tsuchiya K, Jono H, Saito H. 2013. Role of P-glycoprotein in the efflux of raltegravir from human intestinal cells and CD4+ T-cells as an interaction target for anti-HIV agents. *Biochem Biophys Res Commun* 439:221–227. <https://doi.org/10.1016/j.bbrc.2013.08.054>.
 29. van der Galiën R, ter Heine R, Greupink R, Schalkwijk SJ, van Herwaarden AE, Colbers A, Burger DM. 2019. Pharmacokinetics of HIV-integrase inhibitors during pregnancy: mechanisms, clinical implications and knowledge gaps. *Clin Pharmacokinet* 58:309–323. <https://doi.org/10.1007/s40262-018-0684-z>.
 30. Dawes M, Chowienczyk PJ. 2001. Pharmacokinetics in pregnancy. *Best Pract Res Clin Obstet Gynaecol* 15:819–826. <https://doi.org/10.1053/bog.2001.0231>.
 31. Kassahun K, McIntosh I, Cui D, Hreniuk D, Merschman S, Lasseter K, Azrolan N, Iwamoto M, Wagner JA, Wenning LA. 2007. Metabolism and disposition in humans of raltegravir (MK-0518), an anti-AIDS drug targeting the human immunodeficiency virus 1 integrase enzyme. *Drug Metab Dispos* 35:1657–1663. <https://doi.org/10.1124/dmd.107.016196>.
 32. Jeong H, Choi S, Song JW, Chen H, Fischer JH. 2008. Regulation of UDP-glucuronosyltransferase (UGT) 1A1 by progesterone and its impact on labetalol elimination. *Xenobiotica* 38:62–75. <https://doi.org/10.1080/00498250701744633>.
 33. Usui T, Kuno T, Mizutani T. 2006. Induction of human UDP-glucuronosyltransferase 1A1 by cortisol-GR. *Mol Biol Rep* 33:91–96. <https://doi.org/10.1007/s11033-005-1750-9>.
 34. European Medicines Agency. 2007. Isentress: summary of product characteristics. European Medicines Agency, Amsterdam, the Netherlands.
 35. Zheng Y, Aboura R, Boujaafar S, Lui G, Hirt D, Bouazza N, Foissac F, Treluyer J-M, Benaboud S, Gana I. 2020. HPLC-MS/MS method for the simultaneous quantification of dolutegravir, elvitegravir, rilpivirine, darunavir, ritonavir, raltegravir and raltegravir-β-d-glucuronide in human plasma. *J Pharm Biomed Anal* 182:113119. <https://doi.org/10.1016/j.jpba.2020.113119>.
 36. FDA. 2019. Bioanalytical method validation guidance for industry. US Food Drug Administration, Washington, DC.
 37. Fauchet F, Treluyer J-M, Illamola SM, Pressiat C, Lui G, Valade E, Mandelbrot L, Lechedanec J, Delmas S, Blanche S, Warszawski J, Urien S, Tubiana R, Hirt D. 2015. Population approach to analyze the pharmacokinetics of free and total lopinavir in HIV-infected pregnant women and consequences for dose adjustment. *Antimicrob Agents Chemother* 59:5727–5735. <https://doi.org/10.1128/AAC.00863-15>.
 38. Foissac F, Urien S, Hirt D, Frange P, Chaix M-L, Treluyer J-M, Blanche S. 2011. Pharmacokinetics and virological efficacy after switch to once-daily lopinavir-ritonavir in treatment-experienced HIV-1-infected children. *Antimicrob Agents Chemother* 55:4320–4325. <https://doi.org/10.1128/AAC.00166-11>.
 39. Beutler E, Gelbart T, Demina A. 1998. Racial variability in the UDP-glucuronosyltransferase 1 (UGT1A1) promoter: a balanced polymorphism for regulation of bilirubin metabolism? *Proc Natl Acad Sci U S A* 95:8170–8174. <https://doi.org/10.1073/pnas.95.14.8170>.
 40. Rizk ML, Hang Y, Luo W-L, Su J, Zhao J, Campbell H, Nguyen B-Y, Sklar P, Eron JJ, Wenning L. 2012. Pharmacokinetics and pharmacodynamics of once-daily versus twice-daily raltegravir in treatment-naïve HIV-infected patients. *Antimicrob Agents Chemother* 56:3101–3106. <https://doi.org/10.1128/AAC.06417-11>.
 41. Barau C, Furlan V, Yazdanpanah Y, Fagard C, Molina J-M, Taburet A-M, Barrail-Tran A. 2013. Characterization of binding of raltegravir to plasma proteins. *Antimicrob Agents Chemother* 57:5147–5150. <https://doi.org/10.1128/AAC.00625-13>.